

MELT FORMATION AND EVOLUTION ON THE UREILITE PARENT BODY, AS SHOWN BY FELDSPATHIC CLASTS IN POLYMICT UREILITES. C.A. Goodrich,¹ A.H. Treiman¹, and S. Boyle^{1,2}
¹Lunar and Planetary Institute, 3600 Bay Area Blvd, Houston, TX 77058, USA (goodrich@lpi.usra.edu). ²Rutgers University, Dept. Earth and Planetary Sciences, New Brunswick, NJ 08854 USA.

Introduction: Main group ureilites are ultramafic achondrites interpreted to be residues of early partial melting on a common asteroid [1-4]. No known meteorites represent the ureilitic melts, but polymict ureilites, which represent ureilitic regolith, contain a few % feldspathic clasts [2,5-13]. Previous studies of these clasts found that their compositions span the entire range from albite to anorthite, with the most abundant types forming two distinct populations, one with “albitic” plagioclase (An ~0-32) and the other with “labradoritic” plagioclase (An ~33-70) [2,8,9]. From petrology and oxygen isotopes it has been argued that these two groups represent two ureilitic melt lithologies, but their relationship to the main group ureilites or one another has remained unclear [2,8-10]. We have studied > 200 feldspathic clasts in new samples of polymict ureilites, with the goals of better defining the melt lithologies they represent, determining their relationship to main group ureilites, and understanding melt evolution on the ureilite parent body (UPB).

Samples and Methods: We studied >200 feldspathic clasts (~20 μm to 2 mm in size) in 9 thin sections of polymict ureilites Northwest Africa (NWA) 10657, Dar al Gani (DaG) 319, DaG 999, DaG 1000, Frontier Mountain (FRO) 90200 and FRO 03022. X-ray maps of whole sections were used to identify clasts for detailed study. X-ray maps, BEI, and EMP analyses were obtained at ARES, JSC and the Dept. of Geosciences, U. Mass, Amherst.

Results: After eliminating impact melts and foreign clasts [e.g., 9,14], we obtained data for 201 feldspathic clasts. A histogram of average plagioclase An (=molar Ca/[Ca+Na+K]) for 198 of these (3 had feldspathic matrix but no plagioclase) is shown in Fig. 1. As in [8,9,13] the albitic population is the largest, constituting 48% of the clasts studied, while the labradoritic population constitutes 27%. Compared with [8,9,13] we found a significantly higher proportion of calcic (An 70-100) clasts; these may be foreign [10,15] and are discussed elsewhere [16].

The majority of the clasts were simply fragments of plagioclase. Thirty-one of 119 albitic and labradoritic clasts were lithic, consisting of plagioclase (and/or mesostasis) and pyroxene \pm other phases. Mineral chemical parameters for these are given in Fig. 2,3.

All the lithic clasts of the albitic population identified in this work have textures, mineral assemblages and mineral compositions consistent with the albitic

lithology defined by [9,17], i.e., albitic plagioclase, FeO-rich pyroxenes, phosphates, ilmenite, and Fe(Mn,K,P,Ti)-rich glass. They show trends of An vs. Fe/Mg and Fe/Mg vs. Fe/Mn consistent with the fractional crystallization trends of the albitic lithology in [9,17]. Several of the new albitic clasts resemble various textural areas in the Almahata Sitta (ALMA) andesite ALMA-A, supporting the hypothesis that ALMA-A is a hand-sized sample of the albitic lithology [18].

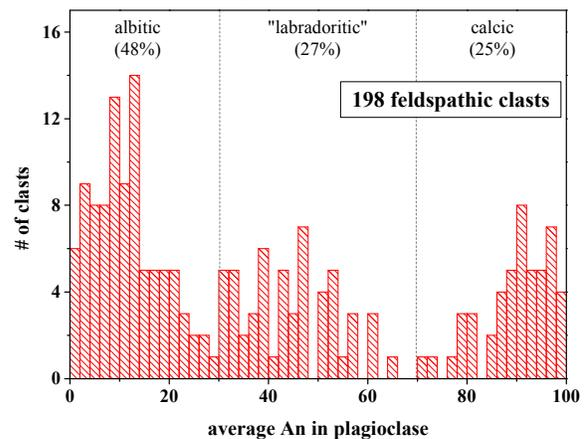


Fig. 1. Histogram of average An content of plagioclase in 198 feldspathic clasts studied. Three distinct populations are evident: albitic (48%), labradoritic (27%), and calcic (25%). The calcic clasts are discussed in [16].

All but two of the labradoritic clasts in this work show magnesian (low Fe/Mg) pyroxene compositions that plot along or near the redox trend of main group ureilite pyroxenes, and are also consistent with the albitic lithology Fe/Mg-Fe/Mn trend (Fig. 3). Several of these show a range of plagioclase compositions extending far into the albitic range (Fig. 2). Of the two labradoritic clasts with ferroan pyroxenes, one plots on the albitic Fe/Mg-Fe/Mn trend (Fig. 3). Only one clast plots along the distinct labradoritic Fe/Mg-Fe/Mn trend of [9] (Fig. 3). This clast (Fig. 4) has An ~64-43 (entirely labradoritic) and very FeO-rich pyroxenes (Fe/Mg = 3-21), with an interstitial SiO₂-rich (~94%), K-poor phase, and minor ulvospinel. This is consistent with [9] that labradoritic clasts did not show incompatible element enrichment as in the albitic lithology.

Discussion: Oxygen isotope compositions ($\Delta^{17}\text{O}$) of albitic and labradoritic clasts previously analyzed are similar to those of the more ferroan (mg# ~78-79) main group ureilites, suggesting that the melts they represent are derived from ferroan source regions on

the UPB [10,19]. However, the Fe/Mg-Fe/Mn trends of the albitic and most of the labradoritic clasts originate on the main group ureilite redox trend at mg# ~90-95 (Fig. 3). This suggests that the melts were reduced by carbon (carried with them?) during ascent [3,21]. However, the supply of carbon must have been limited, and after it was exhausted the melts evolved along normal (near-horizontal) fractionation trends.

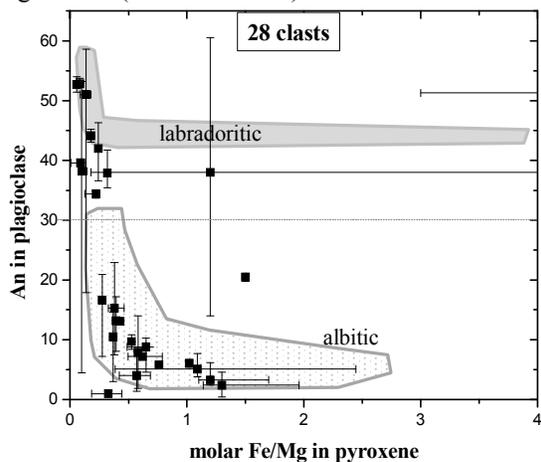


Fig. 2. Molar Fe/Mg in pyroxene vs. An in plagioclase for lithic clasts of the albitic and labradoritic populations in this study, compared with fields (gray and dotted) for these two populations from [9]. Error bars show the range of observed compositions. One labradoritic clast extends to Fe/Mg = 21.

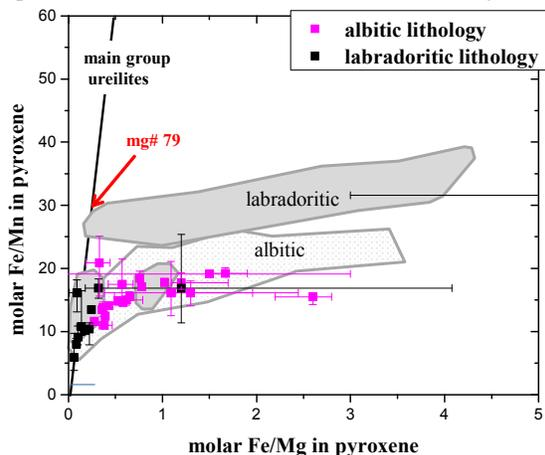


Fig. 3. Molar Fe/Mg vs. Fe/Mn in pyroxene in 30 clasts of the albitic and labradoritic populations in this study, compared with fields from [9] and redox trend of main group ureilites [1,9]. Error bars show range of compositions.

Our new data confirm [8,9,13] that the albitic lithology is the most abundant feldspathic population in polymict ureilites. The highly evolved nature of this lithology is not consistent with it representing a basaltic melt, as would be expected from batch melting. Petrologic modeling simulating fractional melting (in MELTS) suggests that it could be a very early frac-

tional melt (e.g., [21,22]). However, the data in Fig. 2,3 suggest that the magnesian labradoritic clasts might represent a melt that was parental to the albitic lithology and was closer to being basaltic. Alternatively, they may represent a later (more refractory) fractional melt that contained more C than the albitic lithology melt and so was reduced more during ascent.

The distinct labradoritic Fe/Mg-Fe/Mn trend (higher Fe/Mn) in Fig. 3 is defined by only two clasts - DaG 999r clast 10 (Fig. 4) and EET 83309 clast D8 [9]. These clasts may represent a later fractional melt that was not strongly reduced during ascent (due to paucity of C). This is supported by the observation here and in [9] that these clasts (despite high Fe/Mg) do not show the enrichment in incompatible elements seen in the albitic lithology. The relationships between the three lithologies will be further tested using trace element analyses in plagioclase and pyroxene.

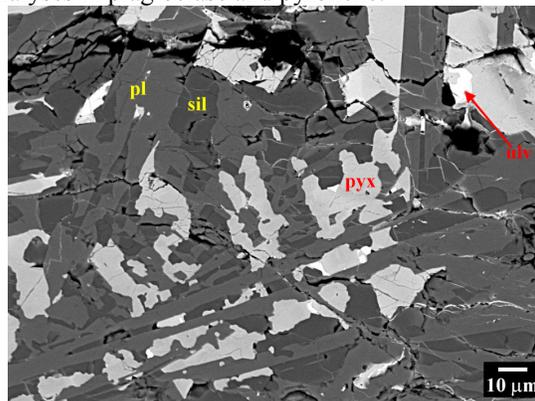


Fig. 4. BEI of DaG 999r clast 10, an extremely ferroan labradoritic clast. This is the only clast from this study that has Fe/Mg-Fe/Mn distinct from the albitic lithology.

References: [1] Mittlefehldt D.W. et al. (1998) In *RIM* 36. [2] Goodrich C.A. et al. (2004) *Chemie der Erde* 64, 283-327. [3] Warren P.H. & Kallemeyn G.W. (1992) *Icarus* 100, 110-126. [4] Scott E.R.D. et al. (1993) *GRL* 20, 415-418. [5] Jaques A.L. & Fitzgerald M.J. (1982) *GCA* 51, 2275-2283. [6] Prinz M. et al. (1987) *LPSC* 18, 802-803. [7] Prinz M. et al. (1988) *LPSC* 19, 947-948. [8] Ikeda Y. et al. (2000) *Ant. Met. Res.* 13, 177-221. [9] Cohen B.A. et al. (2004) *GCA* 68, 4249-4266. [10] Kita N. et al. (2004) *GCA* 68, 4213-4235. [11] Downes H. et al. (2008) *GCA* 72, 4825-4844. [12] Herrin J.S. (2010) *MAPS* 45, 1789-1803. [13] Goodrich C.A. and Wilson L. (2014) *LPSC* 45, #1342. [14] Goodrich C.A. et al. (2016) *LPSC* 47, #1617. [15] Goodrich C.A. et al. (2016) *MSM* 79, #6105. [16] Boyle S. et al. (2017) this meeting. [17] Goodrich C.A. et al. (2010) *EPSL* 295, 531-540. [18] Bischoff A. et al. (2014) *PNAS* 111, 12689-12692. [19] Kita et al. (2006) *MAPS* 41, A96. [20] Wilson L. et al. (2008) *GCA* 72, 6154-6176. [21] Usui T. et al. (2015), *MAPS* 50, 759-781. [22] Gardner-Vandy K. et al. (2014) *LPSC* 45, #1483.